

Miscibility of ionized iron atoms in hydrogen plasmas under the solar interior conditions

Hiroshi Iyetomi and Setsuo Ichimaru

Department of Physics, University of Tokyo, Bunkyo-ku, Tokyo 113, Japan

(Received 8 April 1986)

The generalized hypernetted-chain free-energy formulas derived earlier are used for an accurate analysis of the phase properties in the binary ionic mixtures with dielectric screening of the electrons. The miscibility of iron atoms in the hydrogenic solar plasmas has been treated as a specific example. It is found that while the extent of the electronic screening effect is substantial, the resulting change in the phase diagram is not sufficiently large as to be able to account for the solar-neutrino problem.

I. INTRODUCTION

In an earlier paper,¹ hereafter referred to as paper I, we have derived free-energy formulas applicable to the electron-screened ion plasmas in the hypernetted-chain (HNC) approximation.^{2,3} In the derivation, we have carefully taken account of the density and temperature dependence in the effective interionic potential arising from the static dielectric screening of the electrons. The formulas, expressed in terms of the ion-ion correlation functions and the screening function, enable us to circumvent the more cumbersome and less accurate calculations involving the thermodynamic integrations.

The simplicity and accuracy thereby achieved are valuable in the analyses of phase properties such as miscibilities and phase separations in multi-ionic plasmas. It has now been well established⁴ that a wide variety of binary-ionic mixtures phase separate at lower temperatures. A reliable treatment of such a problem calls for extremely accurate evaluations of the free energies, however, since the characteristics of the phase separation depend on delicate balance between various contributions in the free energies before and after demixing.

In the present paper, we consider such a miscibility problem in hydrogen-iron mixtures under conditions appropriate to the solar interior, as a useful application of the free-energy formulas obtained in paper I. We take the temperatures and the pressures of the solar plasmas in the vicinity of 1.5×10^7 K and 10^5 Mbar. The relative concentration of the irons near the thermonuclear burning region is assumed to take on a value close to the cosmic abundance (2.5×10^{-5} ionic mole fraction).

Highly charged (i.e., high Z) elements are efficient scatterers of the electrons in a plasma, and thus have substantial effects on its transport properties. The solar abundance of high- Z elements such as iron near the thermonuclear burn region can significantly influence the rate of fusion of α particles that generates solar neutrinos being monitored in the ^{37}Cl experiment.^{5,6} Pollock and Alder⁷ in particular have suggested that the solar-neutrino dilemma, a large discrepancy between the observed solar-neutrino counts,⁶ and the calculated capture rates for the standard solar model,⁸ might be resolved, if iron had limited solubility in a hydrogen plasma at the pressures and

temperatures appropriate to the solar interior; a coalescence of irons would lead to the decrease in the opacity and hence the temperature, to suppress those thermonuclear reactions that generate neutrinos detected on the earth. They evaluated the solubility of irons in hydrogen plasmas using the classical Debye-Hückel theory for both electrons and ions, and concluded that the plasma could possibly undergo phase separations at concentrations of irons well below the cosmic abundance.

Following the suggestion of Pollock and Alder, several authors⁹⁻¹¹ advanced refined calculations for the miscibility of irons in solar hydrogen plasmas. Alder, Pollock, and Hansen⁹ treated the interionic correlations in the HNC approximation, and thereby improved on the calculation based on the Debye-Hückel approximation. The Debye-Hückel theory is not valid for the iron-rich phase, where strong coupling effects between ions are crucial; even near the critical point for demixing, accuracy of the Debye-Hückel theory appears insufficient.⁹ On the other hand, Alder *et al.* have completely neglected the electronic screening effects on the thermodynamic properties of the plasmas. They treated the electrons simply as a uniform neutralizing background, and thereby modeled the uniform electron system as a finite-temperature ideal Fermi gas. Pitzer¹⁰ reconsidered Pollock and Alder's analyses, and improved on the short-range behavior of the Debye-Hückel correlation functions phenomenologically. Deutsch, Gombert, and Minoo¹¹ investigated quantum effects of the electrons on the miscibility calculation, based on the nodal expansion method where the bare Coulomb potentials are replaced by their pseudopotentials. All of these investigators have yielded negative answers in resolving the solar-neutrino dilemma through the idea of limited miscibility.

In this paper we revisit the miscibility problem of iron atoms in hydrogen plasmas under the solar-interior conditions, with special emphasis on the role of the electronic screening. Conduction electrons behave semiclassically since the Fermi temperature is somewhat lower than the solar-interior temperature. Such a nondegenerate electron gas acts to screen the ion-ion interaction quite efficiently, and hence modify the thermodynamic properties of the plasma substantially. A possibility may exist, therefore, that the miscibility of irons in the solar hydrogen plasma

is altered significantly by inclusion of the electronic screening effects, leading to a resolution of the solar-neutrino dilemma. We will find through quantitative studies that the extent of the screening effects is indeed substantial but that the resulting change in the phase diagram is not sufficiently large as to be able to account for the solar-neutrino problem.

The present calculations improve over those of Alder, Pollock, and Hansen,⁹ the leading calculations hitherto advanced, in two ways: We take account of the electronic polarization, in the framework of the linear-response theory to the ionic field, assuming that the adiabatic approximation¹² is valid. We also take account of the exchange and correlation contributions to the thermodynamic functions for the electron system, in a way consistent with the screening function of the electrons. The strong coupling effects between ions are treated accurately in the HNC scheme, as Alder, Pollock, and Hansen have done.

In Sec. II we introduce a model of the solar-interior plasma and provide a theoretical framework in which to study the miscibility problem. Section III investigates numerically the electronic screening effects on the correlation properties in solar-interior plasmas. In Sec. IV the phase diagrams for those binary mixtures of the hydrogen-iron plasmas are constructed, and Sec. V summarizes with a conclusion. Some of the calculational details on the phase diagrams are described in the Appendix.

II. FORMULATION OF THE PROBLEM

For simplicity we model the central part of the sun as a three-component plasma consisting of electrons, protons, and ionized iron atoms with electric charge Ze ; such a model has been adopted by many of the previous investigators.^{7,9-11} Under the solar-interior conditions, it has been estimated⁷ that the $1s$ electrons may stay bounded to the iron nuclei while the $2s$ and $2p$ electrons are only partially retained; Z may thus take on a value somewhere between 20 and 24. In this paper we treat a most asymmetric case by assuming $Z=24$; this amounts to consideration of a most favorable situation as far as the proton-iron demixing is concerned.

We consider plasmas consisting of N_1 ions (protons) with charge Z_1e , N_2 ions (irons) with charge Z_2e , and N_e electrons in a volume V at a temperature T . The mean ionic charge is defined as

$$\langle Z^v \rangle = x_1 Z_1^v + x_2 Z_2^v, \quad (1)$$

where $x_1 (= 1 - x_2) \equiv N_1/N$, with $N = N_1 + N_2$. The charge neutrality condition requires $N_e = \langle Z \rangle N$.

We shall describe the state of the plasma in terms of the electronic parameters in the following ways: Defining the Wigner-Seitz radius as $a_e = (3V/4\pi N_e)^{1/3}$, we set the classical Coulomb-coupling constant as^{13,14}

$$\Gamma_e = e^2/a_e k_B T. \quad (2)$$

The dimensionless density parameter¹⁴ is given by

$$r_s = a_e m e^2 / \hbar^2, \quad (3)$$

where m is the mass of an electron. The degree of Fermi

degeneracy is then measured by the ratio θ of the temperature to the Fermi temperature,¹⁴ that is,

$$\theta = 2 \left[\frac{4}{9\pi} \right]^{2/3} r_s / \Gamma_e. \quad (4)$$

The Coulomb coupling constant of the ions may then be given by^{13,14}

$$\Gamma_i = \langle Z^{5/3} \rangle \Gamma_e. \quad (5)$$

In the ensuing calculations we choose r_s and θ as independent variables.

Under the conditions appropriate to the solar interior, those plasma parameters take on values $\Gamma_e \simeq \Gamma_i \simeq 0.05$, $r_s \simeq 0.4$, and $\theta \simeq 4$. This value of Γ_i may suggest that the coupling between ions is generally weak. We nevertheless emphasize the necessity for accurate treatment of the interionic correlations beyond the Debye-Hückel theory, as far as the calculation of the phase diagrams goes; the strongly coupled ionic states are inevitably involved in the iron-rich phase. The electrons, on the other hand, are always in a weakly coupled state. The principal problem on the electrons is to account for the finite-temperature effects appropriately.

If the adiabatic approximation is adopted for the response of the electrons to the ionic field, one can eliminate the electronic coordinates;¹² the system under consideration turns into an electron-screened binary-ionic mixture (BIM).^{13,14} The Fourier transformation of the effective potentials $\phi_{\mu\nu}(r)$ between ions in the linear-response theory is given by

$$\tilde{\phi}_{\mu\nu}(q) = 4\pi Z_\mu Z_\nu e^2 / [q^2 \epsilon(q, 0)], \quad (6)$$

where $\epsilon(q, 0)$ is the static dielectric function of the uniform electron system. The effective potentials thus depend on the number density and temperature of the electrons through $\epsilon(q, 0)$. Since the electrons are weakly coupled, the local-field effects¹⁴ between them can be neglected; $\epsilon(q, 0)$ can be evaluated on the basis of the random-phase approximation (RPA) generalized to the finite electron temperatures.^{14,15} The validity and accuracy of the adiabatic approximation for the electron system in the partially degenerate regime ($\theta \gtrsim 1$) have been investigated in paper I.

The Hamiltonian for the screened BIM now reads

$$H = F_e + K + \frac{1}{2V} \sum_{\mathbf{q} (\neq 0)} v(q) [\rho(\mathbf{q})\rho(-\mathbf{q}) - N \langle Z^2 \rangle] + \frac{1}{2V} \sum_{\mathbf{q} (\neq 0)} v(q) \left[\frac{1}{\epsilon(q, 0)} - 1 \right] \rho(\mathbf{q})\rho(-\mathbf{q}). \quad (7)$$

Here K and F_e represent the kinetic energy of the ions and the Helmholtz free energy of the uniform electron background, respectively; $v(q) = 4\pi e^2/q^2$ is the Fourier transform of the bare Coulomb potential; $\rho(\mathbf{q})$ refers to the Fourier component of the charge-density fluctuations defined as

$$\rho(\mathbf{q}) = Z_1 \rho_1(\mathbf{q}) + Z_2 \rho_2(\mathbf{q}), \quad (8)$$

where $\rho_\sigma(\mathbf{q})$ is the Fourier component of the ion number-density fluctuations of the species σ . As can be readily

seen from the Hamiltonian (7), the thermodynamic functions of the screened BIM consist of three parts,

$$A = A_e + A_{id} + A_{ex}, \quad (9)$$

where A_e is the contribution from the uniform electron gas; A_{id} , the ideal-gas contribution of the ions; A_{ex} , the excess contribution due to the ionic interaction. To be consistent with the choice of $\epsilon(q,0)$ here, we evaluate the thermodynamic functions of the uniform electron system based on the RPA; fitting formulas for the free energies in the RPA (i.e., the exchange and ring contributions) have been obtained by Perrot and Dharma-wardana.¹⁶

Once the laws of interaction between ions are specified, we can calculate various interparticle correlation functions in the screened BIM within the HNC scheme.^{2,3} The accuracy of the HNC approximation in the parameter domain under the present consideration has been confirmed through comparison with molecular dynamics calculations.⁹ The partial pair distribution functions are expressed in the HNC theory as

$$g_{\mu\nu}(r) = \exp\{-[\phi_{\mu\nu}(r)/k_B T] + h_{\mu\nu}(r) - c_{\mu\nu}(r)\}, \quad (10)$$

where $h_{\mu\nu}(r) = g_{\mu\nu}(r) - 1$ refer to the pair correlation functions. The direct correlation functions $c_{\mu\nu}(r)$ are related to $h_{\mu\nu}(r)$ via the Ornstein-Zernike relations,

$$h_{\mu\nu}(r) = c_{\mu\nu}(r) + \sum_{\sigma} x_{\sigma} n \int d\mathbf{r}' c_{\mu\sigma}(|\mathbf{r} - \mathbf{r}'|) h_{\sigma\nu}(r'), \quad (11)$$

where $n = N/V$ is the total number density of ions. The HNC equations (10), coupled with Eq. (11), provide a closed set of equations to be solved for the correlation functions.

The thermodynamic functions for the screened BIM can be expressed in terms of integrals over the correlation functions, in the same way as in the screened one-component plasma case treated in paper I; extension to the BIM case is straightforward. We parametrize $\epsilon(q,0)$ as a function of the dimensionless variables: $Q \equiv q/q_F$, r_s , and θ , where $q_F = (3\pi^2 n_e)^{1/3}$ is the Fermi wave number of the electrons. The excess internal energy and pressure are then calculated as

$$U_{ex} = \frac{n\langle Z^2 \rangle}{2} \sum_{q(\neq 0)} v(q) [S(q) - 1] + \frac{n\langle Z^2 \rangle}{2} \sum_{q(\neq 0)} v(q) \left[\frac{1}{\epsilon(q,0)} - 1 \right] S(q) - \frac{n\langle Z^2 \rangle}{2} \sum_{q(\neq 0)} v(q) \left[\theta \frac{\partial}{\partial \theta} \frac{1}{\epsilon(Q,0)} \right]_{r_s} S(q), \quad (12)$$

$$P_{ex} = \frac{n\langle Z^2 \rangle}{6V} \sum_{q(\neq 0)} v(q) [S(q) - 1] + \frac{n\langle Z^2 \rangle}{6V} \sum_{q(\neq 0)} v(q) \left[\frac{1}{\epsilon(q,0)} - 1 \right] S(q) - \frac{n\langle Z^2 \rangle}{6V} \sum_{q(\neq 0)} v(q) \left[r_s \frac{\partial}{\partial r_s} \frac{1}{\epsilon(Q,0)} \right]_{\theta} S(q) - \frac{n\langle Z^2 \rangle}{3V} \sum_{q(\neq 0)} v(q) \left[\theta \frac{\partial}{\partial \theta} \frac{1}{\epsilon(Q,0)} \right]_{r_s} S(q). \quad (13)$$

Here $S(q)$ denotes the charge-density structure factor of the screened BIM defined as

$$S(q) = \langle \rho(\mathbf{q}) \rho(-\mathbf{q}) \rangle / N \langle Z^2 \rangle. \quad (14)$$

In the framework of the HNC approximation, it is possible to express the Gibbs free energy in terms of the correlation functions without invoking the thermodynamic integration;^{3,17} the scheme has been generalized to the density- and temperature-dependent potential cases in paper I. The excess Gibbs free energy of the screened BIM is thus calculated (in the HNC theory) as

$$G_{ex} = N \sum_{\mu, \nu} x_{\mu} x_{\nu} \left[\frac{nk_B T}{2} \int d\mathbf{r} h_{\mu\nu}(r) [h_{\mu\nu}(r) - c_{\mu\nu}(r)] - nk_B T \bar{c}_{\mu\nu}(q=0) - n \tilde{\phi}_{\mu\nu}(q=0) \right] + \frac{n\langle Z^2 \rangle}{2} \sum_{q(\neq 0)} v(q) \left[\frac{1}{\epsilon(q,0)} - 1 \right] - \frac{n\langle Z^2 \rangle}{6} \sum_{q(\neq 0)} v(q) \left[r_s \frac{\partial}{\partial r_s} \frac{1}{\epsilon(Q,0)} \right]_{\theta} S(q) - \frac{n\langle Z^2 \rangle}{3} \sum_{q(\neq 0)} v(q) \left[\theta \frac{\partial}{\partial \theta} \frac{1}{\epsilon(Q,0)} \right]_{r_s} S(q) - \frac{n\langle Z^2 \rangle}{6} \sum_{q(\neq 0)} v(q) Q \frac{\partial}{\partial Q} \left[\frac{1}{\epsilon(Q,0)} \right] S(q). \quad (15)$$

The excess Helmholtz free energy can then be obtained from Eqs. (13) and (15) with the aid of the standard thermodynamic relation,

$$F_{ex} = G_{ex} - P_{ex} V. \quad (16)$$

The explicit expressions for the partial derivatives of $\epsilon(q,0)$ appearing in Eqs. (12), (13), and (15) have been given in paper I.

III. ELECTRON SCREENING IN THE SOLAR INTERIOR

Before constructing the phase diagram, we examine quantitatively the extent to which the electron screening effects act to modify the correlation properties of solar interior plasmas. For this purpose, we solved the HNC equations for the screened BIM with $Z_1 = 1$ and $Z_2 = 24$ at the solar-interior conditions of $r_s = 0.4$, $\theta = 4$, and

TABLE I. Excess thermodynamic functions for the ionic mixture with $Z_1=1$ and $Z_2=24$ at the conditions of the solar interior ($x_2=2.5 \times 10^{-5}$, $r_s=0.4$, $\theta=4$). BIM refers to the results calculated without electronic screening; screened BIM, those with electronic screening.

	$-\frac{U_{ex}}{Nk_B T}$	$-\frac{P_{ex}}{nk_B T}$	$-\frac{F_{ex}}{Nk_B T}$	$-\frac{G_{ex}}{Nk_B T}$
BIM	0.009 539	0.003 180	0.006 455	0.009 635
Screened BIM	0.016 385	0.005 348	0.011 356	0.016 704

$x_2=2.5 \times 10^{-5}$. Table I lists the excess thermodynamic functions for the screened BIM, together with the BIM results without electronic screening. We find that the relative magnitude of the screening corrections, defined as differences between the screened BIM values and the corresponding BIM values, amounts close to 70%; the electronic screening effect is substantial in the solar interior. In Figs. 1 and 2, we compare the pair distribution functions $g_{\mu\nu}(r)$ and static structure factors $S_{\mu\nu}(q)$ of the BIM with and without the electronic screening. The correlation functions $g_{11}(r)$ and $S_{22}(q)$, omitted in Figs. 1 and 2, stay close to unity. The effect of the electronic screening is evident also in the correlation functions; it thus plays an important part in the determination of the thermodynamic and transport properties in the solar-interior plasmas.

IV. MISCIBILITY OF IRON

Since the phase separation takes place under the conditions of constant pressure and temperature, we deal with the Gibbs free energy of the plasmas, instead of the Helmholtz free energy, to investigate the phase stability.

We begin with defining the Gibbs free energy of mixing as

$$\Delta G(P, T, x_2) = G(P, T, x_2) - x_1 G(P, T, x_2=0) - x_2 G(P, T, x_2=1). \quad (17)$$

If a line can be drawn which is tangential to $\Delta G(x_2)$ curve at two separate points, x_{\min} and x_{\max} , then these points mark the solubility limits at that pressure and temperature; the region between x_{\min} and x_{\max} is unstable

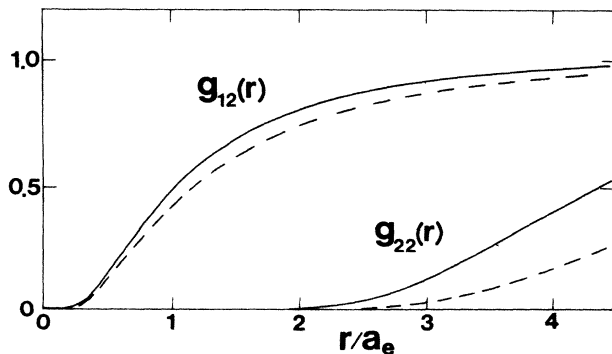


FIG. 1. Partial pair distribution functions for a solar hydrogen-iron mixture at $r_s=0.4$, $\theta=4$, and $x_2=2.5 \times 10^{-5}$. The solid and dashed curves are the results calculated with and without the electronic screening, respectively.

against phase separation into a proton-rich phase at the concentration x_{\min} and an iron-rich phase at the concentration x_{\max} . The critical temperature T_c and the concentration x_c , above which the mixture is always stable, are determined by the two equations

$$\left[\frac{\partial^2 \Delta G}{\partial x_2^2} \right]_{P,T} = 0 \quad (18)$$

and

$$\left[\frac{\partial^3 \Delta G}{\partial x_2^3} \right]_{P,T} = 0. \quad (19)$$

The condition (18) by itself gives the instability (spinodal) curve, which always lies within the coexistence curve determined from the double-tangent construction. We can thus calculate the phase diagrams for the hydrogen-iron mixtures on the basis of the formalism developed in Sec. II; numerical details on the calculation of the phase diagrams are described in the appendix.

As noted earlier, the Gibbs free energy of mixing is expressed as the sum of the electronic, ideal-gas, and excess contributions. We first investigate relative importance of those contributions in the determination of the phase dia-

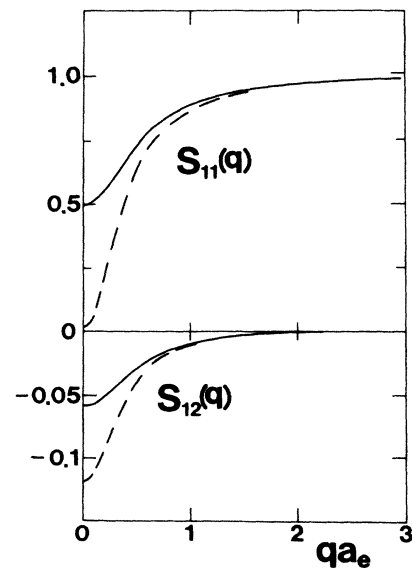


FIG. 2. Partial static structure factors for a solar hydrogen-iron mixture at $r_s=0.4$, $\theta=4$, and $x_2=2.5 \times 10^{-5}$. The notation for the curves is the same as in Fig. 1. Note the difference in scaling above and below the abscissa.

grams. Qualitatively, the electronic and ideal-gas terms favor phase mixing, whereas the excess term promotes phase demixing. In Figs. 3 and 4, we plot the total Gibbs free energy of mixing and the individual contributions as functions of the iron concentration x_2 at two values of the temperature, $T=1.5 \times 10^7$ K and 3.75×10^6 K, at a constant pressure, $P=0.5 \times 10^5$ Mbar. At $T=1.5 \times 10^7$ K, the ideal-gas term is the dominant contribution, and the mixture remains stable against phase separation. As the temperature decreases, however, the magnitudes of the electronic and excess terms increase rapidly; on the other hand, the ideal-gas term remains rather insensitive to the temperature variation. At $T=3.75 \times 10^6$ K, those three contributions take on magnitudes of the same order, where the region of negative curvature,

$$\left(\frac{\partial^2 \Delta G}{\partial x_2^2} \right)_{P,T} < 0, \tag{20}$$

appears. Thus a phase separation of the plasma mixtures takes place as a consequence of delicate balance between those physically distinct contributions.

Figure 5 shows the phase diagram for the hydrogen-iron mixture at $P=0.5 \times 10^5$ Mbar. The solid circles are the calculated points of coexistence; those points are interpolated by the spline method with the third-order polynomials. The critical point for demixing is thus determined at $T_c \simeq 5.5 \times 10^6$ K and $x_c \simeq 2.4 \times 10^{-2}$. The solid triangles are the calculated points of the spinodal; they are similarly interpolated through the critical point determined above. The cross in Fig. 5 denotes the critical point calculated by Alder, Pollock, and Hansen⁹ without consideration of the electronic screening effect. Comparing the present results with those of Alder, Pollock, and Hansen, we find an increase of the critical temperature by

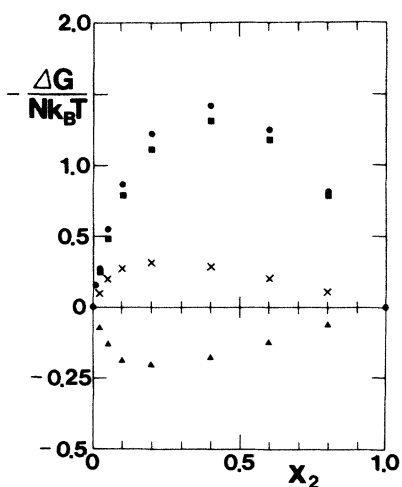


FIG. 3. Contributions to the Gibbs free energy of mixing $\Delta G/Nk_B T$ for the ionic mixture with $Z_1=1$ and $Z_2=24$ at $P=0.5 \times 10^5$ Mbar and $T=1.5 \times 10^7$ K. The points with solid squares represent the ideal-gas contribution; solid triangles, the ionic excess contribution; crosses, the electronic contribution; solid circles, sum of all the three contributions. Note the difference in scaling above and below the abscissa.

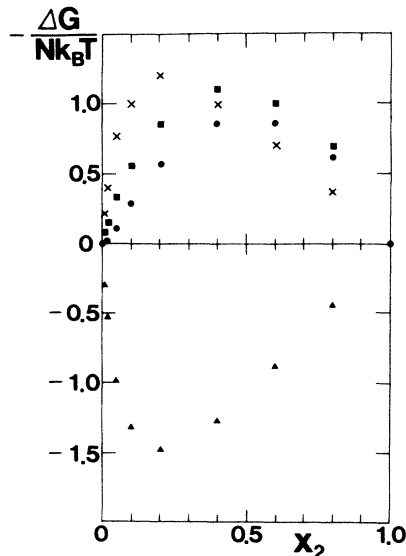


FIG. 4. Same as Fig. 3, but at $T=3.75 \times 10^6$ K.

15% arising from the electronic screening effect. The absolute value of the critical temperature is still smaller than the solar-interior temperature, however, by a factor of less than a half. Consequently, we may conclude that an accurate treatment of the miscibility problem, as presented here, has not revealed a new possibility of resolving the solar-neutrino dilemma through the idea of a limited solu-

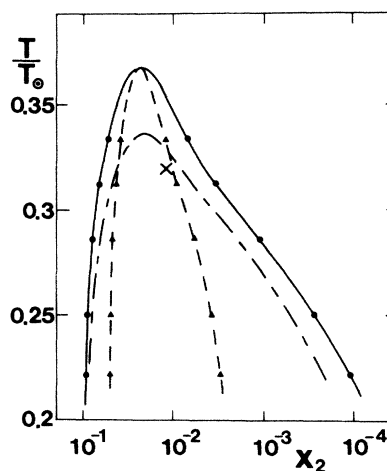


FIG. 5. Phase diagrams for the H^+-Fe^{24+} mixture with the electronic screening at $P=0.5 \times 10^5$ Mbar. The temperature T in the ordinate is normalized with $T_{\odot}=1.5 \times 10^7$ K, the interior temperature of the sun. The solid and dashed curves are the coexistence and spinodal curves, interpolated as described in the text; the solid circles and triangles represent the calculated points. The cross refers to the critical point obtained without the electronic screening by Alder, Pollock, and Hansen (Ref. 9). The chain curve is the coexistence curve calculated by retaining only the ideal-gas term in the equation of state for the uniform electron gas.

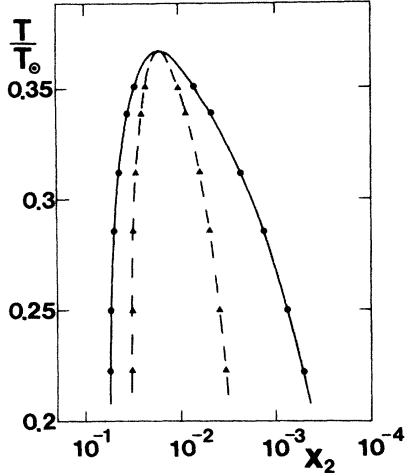


FIG. 6. Same as Fig. 5, but at $P=10^5$ Mbar.

bility of the iron atoms in the solar-interior plasma.

To see how the adopted electronic equation of state may influence the phase diagram, we have performed an additional calculation of the coexistence curve by taking only the ideal-gas term in A_e . The result is shown in Fig. 5 by a chain curve. We find that the neglected terms in A_e , i.e., the exchange and ring contributions, affect substantially, in that the change of the critical temperature amounts to about 10%.

We have also calculated the phase diagram for the hydrogen-iron mixture at $P=10^5$ Mbar; the result is shown in Fig. 6. The critical point for demixing is $T_c \simeq 5.5 \times 10^6$ K and $x_c \simeq 1.7 \times 10^{-2}$. Although the critical point is located at about the same place as in Fig. 5, the increase of pressure appears to result in prevention of phase separation at lower temperatures ($T \leq 0.3T_\odot$). The suppression of phase demixing at an elevated pressure may be accounted for as follows: In that temperature domain where the electrons are moderately degenerate ($\theta \lesssim 1.0$), an increase in the pressure corresponds to an increase in the charge density or a decrease in r_s , so that the uniform electron system looks more like a rigid background; ionic mixtures in such a background have been shown¹⁷ to be stable against phase separation.

V. CONCLUSION

We have shown the use of the generalized HNC free-energy formula for an accurate analysis of the phase properties in the ionic mixtures with electronic screening. The problem of the iron miscibility in the hydrogenic solar plasma has been treated as a concrete example, with the hope of shedding light on the solution to the solar-neutrino problem. The temperatures at which the solubility of the iron atoms is limited have turned out to be significantly lower than the solar-interior temperature, so that the idea of limited solubility does not appear capable of resolving the solar-neutrino dilemma.

ACKNOWLEDGMENTS

This research was supported in part through a Grant-in-Aid for Scientific Research, No. 59380001, provided by the Japanese Ministry of Education, Science, and Culture.

APPENDIX: CALCULATION OF THE PHASE DIAGRAMS

For the calculation of the phase diagrams, it is useful to have an analytic expression for the Gibbs free energy of the plasma at a given P and T as a function of the concentration x_2 . In the present calculations, we have derived such an expression for the Gibbs free energy in the following way.

To begin, we establish a one-to-one correspondence between a set of the plasma parameters (r_s, θ) and a given combination of the thermodynamic variables (P, T) regarding x_2 as a variable parameter; the thermodynamic functions for the plasma are expressible as functions of r_s, θ , and x_2 . When the temperature is fixed, the parameter r_s is related to θ via the relation,

$$r_s = 762.61 \left[\frac{\theta}{T[\text{K}]} \right]^{1/2}, \quad (\text{A1})$$

so that the correspondence is established once θ is expressed as a function of P through the equation of state. To do so, we have computed the pressure as a function of θ for 17 values of x_2 including the end points, and fitted the computed values by a polynomial of $\ln\theta$ as

$$P = \sum_k a_k (\ln\theta)^k. \quad (\text{A2})$$

At the same time, we calculate the excess Gibbs free energies and fit the resulting values in a similar polynomial form,

$$G_{\text{ex}} = \sum_k a'_k (\ln\theta)^k. \quad (\text{A3})$$

The formulas (A2) and (A3) with the first five terms can fit the original values within the accuracy of 0.2%. Using Eqs. (A2) and (A3), we obtain the values of θ and G_{ex} for the 17 values of x_2 at a given specification of P and T .

We then parametrize those results obtained above as functions of x_2 , using a (3-2) Padé approximant,

$$\theta(x_2) = \frac{a + bx_2 + cx_2^2 + dx_2^3}{1 + ex_2 + fx_2^2}, \quad (\text{A4})$$

$$G_{\text{ex}}(x_2) = \frac{a' + b'x_2 + c'x_2^2 + d'x_2^3}{1 + e'x_2 + f'x_2^2}. \quad (\text{A5})$$

Four of the six free parameters in (A4) are determined from the exact limiting behaviors,

$$\lim_{x_2 \rightarrow 0} \theta(x_2) = \theta(x_2=0) + \frac{\partial\theta}{\partial x_2}(x_2=0)x_2 + \cdots, \quad (\text{A6})$$

$$\lim_{x_2 \rightarrow 1} \theta(x_2) = \theta(x_2=1) + \frac{\partial\theta}{\partial x_2}(x_2=1)(x_2-1) + \cdots, \quad (\text{A7})$$

where we evaluate the first derivatives of θ in x_2 numerically. The remaining two parameters are then determined, so as to minimize the difference between the original and fitted values; the resulting fitting errors are confined within 0.2%. The parameters in the fitting formula (A5) for G_{ex} are determined analogously, with errors on the same order of magnitude.

The ideal-gas contribution to ΔG is written explicitly as¹⁸

$$\frac{\Delta G_{id}}{Nk_B T} = x_1 \ln \left[\frac{x_1 Z_1}{\langle Z \rangle} \frac{r_s^3(x_2=0)}{r_s^3(x_2)} \right] + x_2 \ln \left[\frac{x_2 Z_2}{\langle Z \rangle} \frac{r_s^3(x_2=1)}{r_s^3(x_2)} \right], \quad (\text{A8})$$

where $r_s(x_2)$ is the r_s value at x_2 for a given specification of P and T . One derives an analytic expression for the electronic contribution to ΔG as a function of r_s and θ , following Perrot and Dharma-wardana's formulas.¹⁶ The equations (A4) and (A5), together with Eq. (A1), thus provide the desired analytic expression for ΔG as a function of x_2 at a given specification of P and T ; this result facilitates the procedure of double-tangent construction and the evaluation of the spinodal points. We remark in passing that major parts of the free-energy contributions cancel each other in the calculation of ΔG via Eq. (17); the errors in ΔG calculated from the analytic expression may have reached several percent.

¹H. Iyetomi and S. Ichimaru, *Phys. Rev. A* **34**, 433 (1986).

²J. M. J. Van Leeuwen, J. Groeneveld, and J. De Boer, *Physica (Utrecht)* **25**, 792 (1959).

³T. Morita, *Prog. Theor. Phys.* **23**, 829 (1960).

⁴See, e.g., J. P. Hansen, *J. Phys. (Paris) Colloq.* **41**, C2-43 (1980).

⁵See, J. N. Bahcall and R. K. Ulrich, *Astrophys. J.* **170**, 593 (1971), and the references therein.

⁶R. Davis, Jr., *Bull. Am. Phys. Soc.* **29**, 731 (1984).

⁷E. L. Pollock and B. J. Alder, *Nature* **275**, 41 (1978).

⁸J. N. Bahcall, W. F. Huebner, S. H. Lubow, P. D. Parker, and R. K. Ulrich, *Rev. Mod. Phys.* **54**, 767 (1982).

⁹B. J. Alder, E. L. Pollock, and J. P. Hansen, *Proc. Natl. Acad. Sci. USA* **77**, 6272 (1980).

¹⁰K. S. Pitzer, *Proc. Natl. Acad. Sci. USA* **77**, 3103 (1980).

¹¹C. Deutsch, M. M. Gombert, and H. Minoo, *J. Phys. (Paris)*

Colloq. **41**, C2-65 (1980); M. M. Gombert and C. Deutsch, *Phys. Scr.* **T7**, 113 (1984).

¹²N. W. Ashcroft and D. Stroud, in *Solid State Physics* (Academic, New York, 1978), Vol. 33, p. 1.

¹³M. Baus and J. P. Hansen, *Phys. Rep.* **59**, 1 (1980).

¹⁴S. Ichimaru, *Rev. Mod. Phys.* **54**, 1017 (1982).

¹⁵J. Lindhard, *K. Dan. Vidensk. Selsk. Mat.-Fys. Medd.* **28**, 8 (1954).

¹⁶F. Perrot and M. W. C. Dharma-wardana, *Phys. Rev. A* **30**, 2619 (1984).

¹⁷J. P. Hansen, G. M. Torrie, and P. Vieillefosse, *Phys. Rev. A* **16**, 2153 (1977).

¹⁸B. Brami, J. P. Hansen, and F. Joly, *Physica (Utrecht) A* **95**, 505 (1979).